

On the Redundant Carrier Distribution for UW-OFDM

Heidi Steendam

DIGCOM research group, TELIN Dept., Ghent University

E-mail: Heidi.Steendam@telin.ugent.be

Abstract—Unique word (UW) OFDM is a new multicarrier technique that was first introduced in [1]. In this technique, the guard interval is a part of the inverse FFT (IFFT) output, and is filled with known symbols. To be able to construct – by using an IFFT – a time domain signal containing a block of known samples, it is necessary to sacrifice a number of carriers. These carriers are called redundant carriers and the symbols modulated on these redundant carriers depend on the data to be transmitted. In this paper, we evaluate the distribution of the redundant carriers over the bandwidth. It turns out that when the positions of the redundant carriers are not carefully selected, the extra energy needed for the redundant carriers can become very large. We propose a novel algorithm for the placement of the redundant carriers that is based on a simple analytical expression, such that extensive simulations to find the optimal distribution is avoided. The proposed distribution yields essentially minimal average redundant energy.

I. INTRODUCTION

The success of multicarrier systems like OFDM can be attributed to their robustness to channel dispersion and their high bandwidth efficiency [2]. This makes them the best candidate for various applications, witness the different standards that use multicarrier transmission as (one of) its basic modulation techniques, e.g. [3]-[4]. In order to avoid intersymbol interference caused by overlap in the time domain of sequentially transmitted OFDM blocks, typically a guard interval is inserted between the different IFFT blocks. In the literature, different guard interval techniques can be found, e.g. cyclic prefix, zero padding and known symbol padding [5]-[6] – the cyclic prefix technique however is the most popular of these techniques. In these traditional guard interval techniques, the guard interval is not a part of the IFFT block, i.e. the length of the OFDM symbol is extended. Recently, a new OFDM technique was introduced, i.e. unique word OFDM (UW-OFDM) [1]. In contrast with the traditional guard interval techniques, in UW-OFDM, the guard interval is a part of the IFFT block: the last part of the IFFT block is a block of known samples, called the unique word. The construction of the unique word requires that part of the carriers cannot be used for data transmission but contain a linear combination of the symbols transmitted on the data carriers. Hence, UW-OFDM introduces redundancy in the frequency domain.

In [7], the two-step approach to construct UW-OFDM was introduced. In this approach, first a block of zero samples is constructed at the positions of the unique word by properly selecting the information modulated on the redundant carriers, and in the second stage, the known samples of the unique

word are added. As in this method, first a signal with a block of zeros in the time domain is constructed, the UW-OFDM technique can be compared with a Reed-Solomon code [8]. Comparing CP-OFDM with UW-OFDM, it follows that the throughput efficiency for UW-OFDM is lower than for CP-OFDM, e.g. for a guard interval length equal to 25% of the FFT length, the throughput efficiency for CP-OFDM is 80% whereas for UW-OFDM, it is only 75%. This follows from the fact that in the latter, the guard interval is a part of the IFFT block, whereas in the former it is not. Hence, the relative reduction of the throughput efficiency in UW-OFDM is larger. This implies that in an AWGN channel, the CP-OFDM will outperform UW-OFDM in terms of BER (this effect was shown in [7]). However, it was shown in [7] for uncoded and in [1], [9] for coded OFDM that in the presence of frequency selective channels, UW-OFDM outperforms CP-OFDM in terms of BER. This implies that the redundancy in the frequency domain from UW-OFDM results in a coding gain as compared to CP-OFDM – a coding gain that becomes larger when the channel contains more deep fades. Note that in CP-OFDM deep fades can be counteracted with precoding resulting in coded OFDM (COFDM) [10]-[12]. However, precoded OFDM needs the availability of channel state information (CSI) at the transmitter side – which is not always easy to obtain, whereas in UW-OFDM no CSI is necessary.

In [1] and [7], the authors restricted their attention to the case where the number of redundant carriers equals a power of two. In [13] it is analytically shown that the optimal placement of the redundant carriers in that case is the uniform distribution¹. In this paper, we would like to extend this to the general case, where the number of carriers is not necessarily a power of 2. This will provide an extra degree of freedom in the design of UW-OFDM. However, we show in this paper that when the positions of the redundant carriers are not carefully selected, the average energy needed for these redundant carriers can increase exponentially. Hence, it is of major importance to determine an appropriate redundant carrier distribution. In this paper, we propose a novel redundant carrier distribution that places the redundant carriers using a simple analytical algorithm, such that extensive simulations to

¹Note that the optimal distribution found in [1] and [7] through simulations is not entirely uniform. This is because in these papers, a guard band is considered where no data or redundant carriers can be placed. This influences the optimal placement of the redundant carriers.

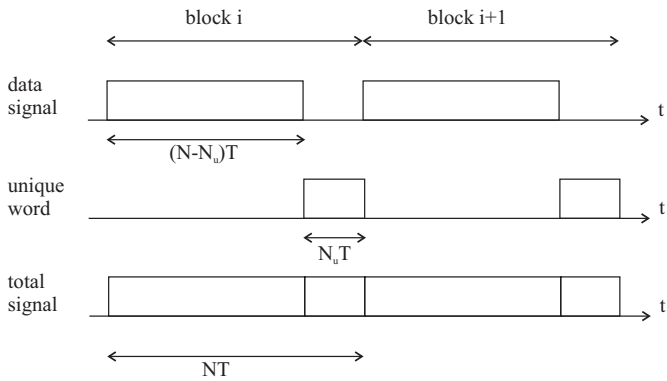


Fig. 1. Time-domain structure of UW-OFDM.

find the optimal distribution as in [1] are no longer required. We compare the average redundant energy needed for the proposed distribution with those for other distributions, and show that the proposed distribution results in essentially the minimal average redundant energy.

II. SYSTEM DESCRIPTION

The time-domain structure of the UW-OFDM signal is shown in figure 1. A block contains N time domain samples generated at a sample rate $1/T$. The first $N - N_u$ samples correspond to the data, and the last N_u samples form the unique word with the known samples. In the first step of the two-step approach from [7], first a block of N_u zeros is constructed in the time domain. This is achieved by selecting N_r redundant carriers, where it is required that $N_r \geq N_u$. The time-domain signal in this first step is given by

$$\mathbf{y} = \mathbf{F}_N^{-1} \mathbf{P} \begin{pmatrix} \mathbf{x}_d \\ \mathbf{x}_r \end{pmatrix}, \quad (1)$$

where $\mathbf{x}_d = (x_d(1) \dots x_d(N - N_r))^T$ are the $N - N_r$ data symbols, $\mathbf{x}_r = (x_r(1) \dots x_r(N_r))^T$ the N_r redundant symbols, \mathbf{F}_N is the $N \times N$ FFT matrix with $(\mathbf{F}_N)_{k,\ell} = \frac{1}{\sqrt{N}} e^{-j2\pi \frac{k\ell}{N}}$ and \mathbf{P} is the permutation matrix. The $N \times N$ permutation matrix \mathbf{P} determines the positions of the data and redundant carriers and can be decomposed as $\mathbf{P} = [\mathbf{P}_d \quad \mathbf{P}_r]$, where \mathbf{P}_d is $N \times N_d$ and \mathbf{P}_r $N \times N_r$. The columns of \mathbf{P} are unit vectors; the '1' in the unit vectors from \mathbf{P}_d are at the positions $\tilde{n}_\ell \in I_d$, where I_d is the set of N_d data carrier positions, and at the positions $n_\ell \in I_r$ for the matrix \mathbf{P}_r , where I_r is the set of N_r redundant carrier positions.

The transform matrix \mathbf{M} is defined as $\mathbf{M} = \mathbf{F}_N^{-1} \mathbf{P}$ and can be decomposed as

$$\mathbf{M} = \begin{pmatrix} \mathbf{M}_{11} & \mathbf{M}_{12} \\ \mathbf{M}_{21} & \mathbf{M}_{22} \end{pmatrix}, \quad (2)$$

where \mathbf{M}_{11} is $(N - N_u) \times N_d$, \mathbf{M}_{12} is $(N - N_u) \times N_r$, \mathbf{M}_{21} is $N_u \times N_d$ and \mathbf{M}_{22} is $N_u \times N_r$. Imposing that the last N_u time domain samples must be zero results in a set of linear equations $\mathbf{M}_{21} \mathbf{x}_d + \mathbf{M}_{22} \mathbf{x}_r = \mathbf{0}$. The solution with minimum average redundant energy $P_r = E[\mathbf{x}_r^H \mathbf{x}_r]$ is given by

$$\mathbf{x}_r = -\mathbf{M}_{22}^\dagger \mathbf{M}_{21} \mathbf{x}_d = \mathbf{T} \mathbf{x}_d, \quad (3)$$

where $\mathbf{M}_{22}^\dagger = \mathbf{M}_{22}^H (\mathbf{M}_{22} \mathbf{M}_{22}^H)^{-1}$ is the Penrose-Moore pseudo-inverse. This results in the time-domain signal:

$$\mathbf{y} = \mathbf{M} \begin{pmatrix} \mathbf{I}_{N_d} \\ \mathbf{T} \end{pmatrix} \mathbf{x}_d = \mathbf{G} \mathbf{x}_d, \quad (4)$$

where \mathbf{I}_{N_d} is the $N_d \times N_d$ identity matrix. The last N_u rows of the matrix \mathbf{G} are zero rows.

Assuming $E[x_d(i)x_d^*(j)] = E_s \delta_{i,j}$ is the energy of a data symbol, it follows that the average energy of the time domain samples is given by

$$P_t = E[\mathbf{y}^H \mathbf{y}] = P_d + P_r, \quad (5)$$

where $P_d = E_s N_d$ is the average data energy and $P_r = E_s \text{trace}(\mathbf{T}^H \mathbf{T})$ the average redundant energy. To obtain a high power efficiency, it is of importance that the average energy of the redundant symbols is as small as possible. Taking into account (3), the average redundant energy can be rewritten as

$$P_r = E_s \text{trace}[\mathbf{M}_{21} \mathbf{M}_{21}^H (\mathbf{M}_{22} \mathbf{M}_{22}^H)^{-1}]. \quad (6)$$

The optimal distribution is the distribution that minimizes the average redundant energy P_r . In the special case where N_r is a power of 2, it is shown in [13] that a uniform distribution of the redundant carriers over the bandwidth results in the minimum average redundant energy. Defining the spacing between the redundant carriers as $\Delta = N/N_r$, the redundant carrier indices in that case are given by $n_\ell = n_0 + \ell\Delta$, $\ell = 0, \dots, N_r - 1$ and $0 \leq n_0 < \Delta$. When N_r is no longer a power of 2, the situation becomes more complex. We show in the simulations that in this latter case, the uniform distribution is no longer optimal. The contrary occurs: a uniform distribution with carrier spacing $\Delta = \lfloor \frac{N}{N_r} \rfloor$ results in some cases in an 'explosion' of the average redundant power. An explanation for this can be found in (6): in some cases, the uniform distribution makes the matrix $\mathbf{M}_{22} \mathbf{M}_{22}^H$ become (close to) singular.

It turns out that the average redundant energy strongly depends on the positions of the redundant carriers. For the general case where N_r is not a power of 2, we have carried out an exhaustive search to find the optimum distribution of the redundant carriers for $N \leq 32$; for $N > 32$, an exhaustive search was infeasible because of the computational load. The optimum positions of the redundant carriers depended on the system parameters N , N_r and N_u , but no simple rule of thumb could be found to extend the results to general values of N , N_r and N_u . To avoid the computational burden to find the optimal distribution every time the system parameters are changed, we prefer a (suboptimal) distribution that selects the redundant carrier positions according to a simple analytical expression.

In this paper, we propose the following redundant carrier distribution. This 'split' carrier distribution avoids the matrix $\mathbf{M}_{22} \mathbf{M}_{22}^H$ to become singular, and in the simulations, we show that this distribution yields for many values of N_r the lowest average redundant energy. Assume the number N_r of redundant carriers can be written as the following sum of

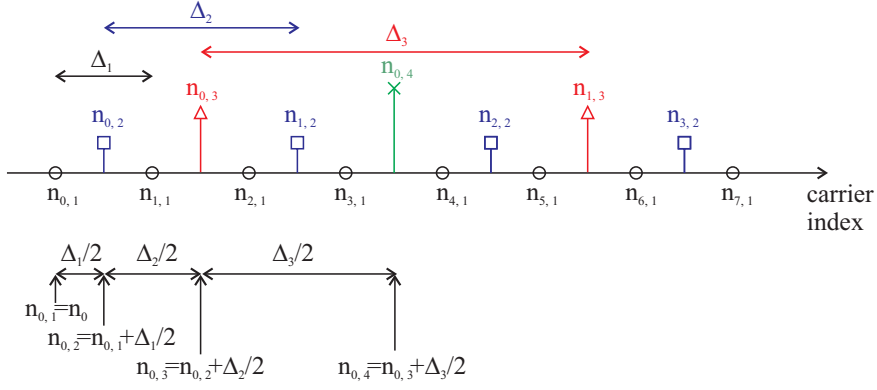


Fig. 2. Proposed redundant carrier distribution for $N_r = 15$: $N_{r,1} = 8$, $N_{r,2} = 4$, $N_{r,3} = 2$, $N_{r,4} = 1$. The spacings equal $\Delta_1 = \frac{\Delta_2}{2} = \frac{\Delta_3}{4}$.

powers of 2:

$$N_r = \sum_{\ell=1}^{L_r} N_{r,\ell}, \quad (7)$$

where $N_{r,\ell} = 2^{x_\ell}$, x_ℓ is integer and $N_{r,1} > N_{r,2} > \dots > N_{r,L_r}$. We split the set I_r of N_r redundant carriers in L_r sets $I_{r,\ell}$ with $N_{r,\ell}$ redundant carriers. Within each set $I_{r,\ell}$, the positions of the $N_{r,\ell}$ redundant carriers are uniformly distributed over the bandwidth with spacing $\Delta_\ell = \frac{N}{N_{r,\ell}}$, resulting in the carrier indices

$$n_{m,\ell} = n_{0,\ell} + m\Delta_\ell, \quad m = 0, \dots, N_{r,\ell} - 1. \quad (8)$$

The offsets $n_{0,\ell}$ of the carrier positions within the different sets $I_{r,\ell}$ must be carefully selected in order that the matrix $\mathbf{M}_{22}\mathbf{M}_{22}^H$ is not singular. The following choice for the offsets yielded the minimal energy of the redundant symbols:

$$\begin{aligned} n_{0,1} &= n_0 \\ n_{0,\ell} &= n_{0,\ell-1} + \frac{\Delta_{\ell-1}}{2} + m_\ell \Delta_{\ell-1}, \quad \ell > 1, \end{aligned} \quad (9)$$

where $0 \leq n_0 < \Delta_1$ and m_ℓ is integer². Assuming $m_\ell = \frac{N_{r,\ell-1}}{2N_{r,\ell}} - 1$, $\forall \ell > 1$ the offsets $n_{0,\ell}$ can be rewritten as $n_{0,\ell} = n_0 + \frac{N}{2N_{r,\ell}} - \frac{N}{2N_{r,1}}$. In figure 2, the distribution is shown for the case where $N_r = 15$, assuming $m_\ell = 0$. Note that, when N_r is a power of 2, the proposed distribution results in a uniform distribution of the redundant carriers over the bandwidth.

III. NUMERICAL RESULTS

In this section, we evaluate the distribution of the redundant energy $\mathbf{x}_r^H \mathbf{x}_r$ by means of a histogram for the following redundant carrier distributions. The average redundant energy P_r can be extracted from the histograms by averaging over the redundant energy $\mathbf{x}_r^H \mathbf{x}_r$. The first distribution is the uniform distribution, where the redundant carriers are evenly spread over the bandwidth. Assuming N_r redundant carriers, the carrier spacing equals $\Delta = \lfloor \frac{N}{N_r} \rfloor$, and the positions of the

²It can easily be verified that a shift of $n_{0,\ell}$ over a multiple of $\Delta_{\ell-1}$ has no influence on the average redundant energy. This is an interesting property when dealing with a system with guard bands: in this way we can avoid carriers that are not allowed to be used.

redundant carriers are $n_\ell = n_0 + \ell\Delta$, $\ell = 0, \dots, N_r - 1$ with $0 \leq n_0 < \Delta$. The second distribution is the random distribution, where the redundant carriers are randomly spread over the bandwidth, and the third distribution is the proposed 'split' distribution. The redundant energy is shown in histograms generated based on 10000 Monte Carlo simulations, where the data symbols are randomly generated QPSK symbols. Further, we restrict our attention to the case where $N_u = N_r$ and $N = 128$. However, simulations have shown that when $N_r > N_u$ or for other values of N , the results are similar.

Figure 3 shows the histogram of the redundant energy $\mathbf{x}_r^H \mathbf{x}_r$ for the uniform distribution, assuming the offset n_0 is fixed for all simulations ($n_0 = 0$), for different values for N_r . Note that the abscissa of the histogram is logarithmic. For small values of N_r , the histogram shows a sharp peak around $\mathbf{x}_r^H \mathbf{x}_r = NE_s$. Increasing N_r , however, moves the redundant energy and hence the average redundant energy P_r to larger values: while for $N_r = 5$, the average redundant energy is approximately NE_s , the redundant energy has increased to approximately $100NE_s$ for $N_r = 30$. Hence, it is clear that the uniform distribution is not optimal for larger values of N_r . In figure 4, the effect of the offset n_0 is shown: in this case, for each of the simulations, the offset is randomly picked from a uniform distribution in the interval $0 \leq n_0 < \Delta$. From the figure, when comparing the curve for a fixed n_0 and a randomly selected n_0 , it is clear that the offset has no influence on the (average) redundant energy.

In figure 5, the results are shown for a random distribution, where for each simulation, the positions of the redundant carriers are independently changed. Comparing the results from figures 3 and 5, it follows that the (average) redundant energy in the random case is much higher than for the uniform distribution: there are values for the redundant energy in the histogram in figure 5 that are several orders of magnitude larger than NE_s . Hence, a complete random distribution for the positions of the redundant carriers is clearly not optimal. Therefore, we followed in figure 6 the following strategy. Based on 10000 Monte Carlo simulations, we selected the redundant carrier distribution that yielded the smallest redundant energy. Using this 'optimal' random distribution, another

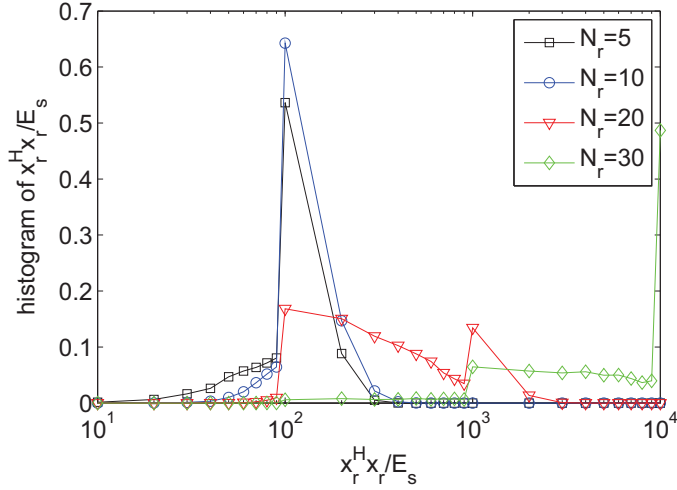


Fig. 3. Histogram of the redundant energy for the uniform distribution $N = 128$, $N_u = N_r$, offset n_0 fixed.

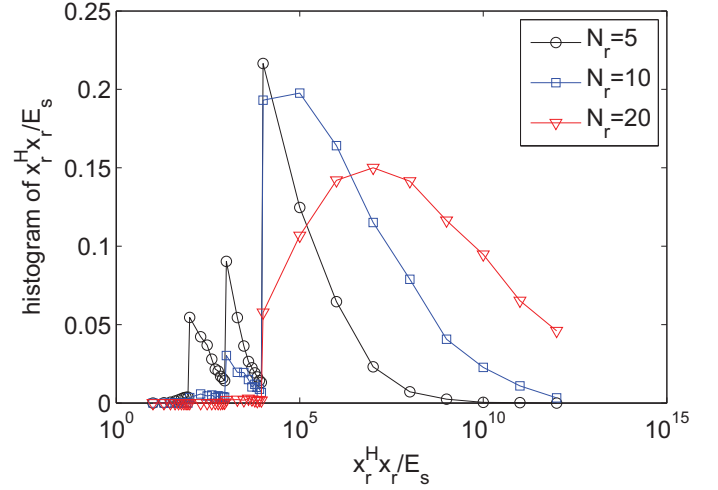


Fig. 5. Histogram of the redundant energy for the random distribution $N = 128$, $N_u = N_r$.

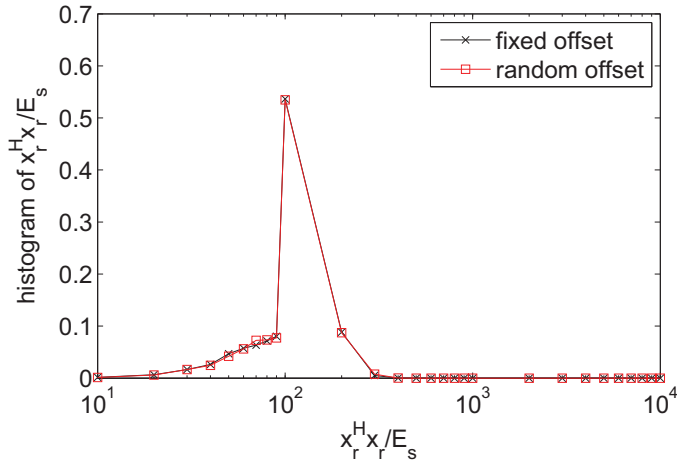


Fig. 4. Histogram of the redundant energy for the uniform distribution $N = 128$, $N_u = N_r = 5$ for fixed and random offset n_0 .

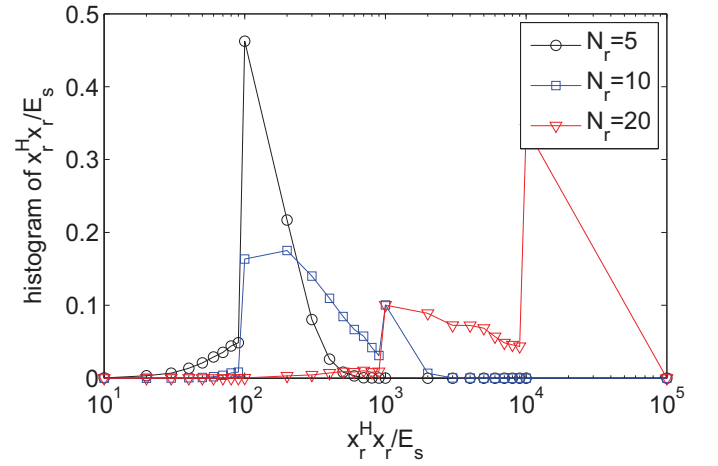


Fig. 6. Histogram of the redundant energy for the optimal random distribution $N = 128$, $N_u = N_r$.

10000 Monte Carlo simulations were executed, resulting in figure 6. Comparing figures 5 and 6, a large gain is obtained. However, comparing figures 3 and 6 shows that the uniform distribution still performs better than the optimal random distribution.

The results for the proposed split distribution are shown in figure 7 for a fixed offset $n_0 = 0$. Simulations have shown that, similarly as for the uniform distribution, the offset has no effect on the average redundant energy. We observe for all values of N_r a sharp peak in the histogram at approximately NE_s . Increasing N_r makes this peak sharper and moves the (average) redundant energy to lower values. Hence, the proposed split distribution avoids the 'explosion' of the needed (average) redundant energy observed for the uniform and random distributions. On the contrary: increasing N_r for the split distribution even reduces the variance of the redundant energy! Although for small values of N_r , the (average) redundant

energy for the split distribution is somewhat larger than for the uniform distribution (compare figures 3 and 7), it can be concluded that the proposed distribution gives rise to the best results: for this distribution, the (average) redundant power is essentially minimal.

From the results of the split distribution, it can be observed that the average energy needed for the redundant carriers (this approximately corresponds to the peak in the histogram) is of the order of the energy needed to transmit the data symbols. Hence, UW-OFDM essentially doubles the energy needed to transmit N_d data symbols. This does not take into account the energy needed for the unique word itself! So at a first sight, UW-OFDM is very energy inefficient. However, this extra energy is used to create redundancy in the signal, as in an error correcting code. At the receiver, using a data detector that fully exploits all redundancy available in the signal will transform this extra energy into a sort of 'coding gain', hence

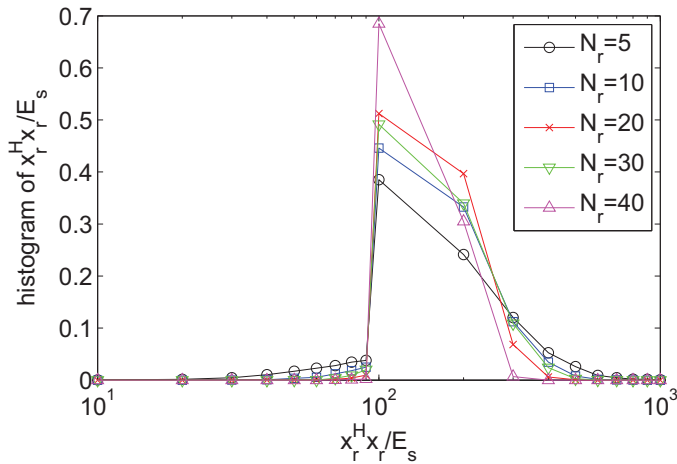


Fig. 7. Histogram of the redundant energy for the split distribution $N = 128$, $N_u = N_r$, offset n_0 fixed.

the loss in power efficiency is compensated.

IV. CONCLUSIONS

In this paper, we evaluated the effect of different distributions for the redundant carriers on the (average) energy needed for the redundant symbols. In [13], it was shown that the optimal distribution in the case that N_r is a power of 2 is the uniform distribution. In this paper, we have extended the results for values of N_r that are not a power of 2. In this general case, we have shown that the uniform distribution of the redundant carriers is no longer optimal. To the contrary, a uniform distribution will give rise to an enormous increase in the necessary energy for various values of N_r . To overcome this growth in the necessary redundant energy, we proposed a novel distribution for the positions of the redundant carriers, based on a simple analytical expression. The proposed distribution reduces to the uniform distribution when N_r is a power of 2, and can hence be seen as a natural extension of the uniform distribution for general values of N_r . In the simulations, it is shown that this distribution does not increase the required (average) redundant energy, and will need essentially the minimal energy of the considered distributions.

ACKNOWLEDGEMENT

The author gratefully acknowledges the financial support from the Flemish Fund for Scientific Research (FWO).

REFERENCES

- [1] M. Huemer, C. Hofbauer, J. B. Huber, "The Potential of Unique Words in OFDM," in Proc. InOWo'10, Hamburg, Germany, Sep 2010, pp. 140–144.
- [2] J. A. C. Bingham, "Multicarrier Modulation for Data Transmission, an Idea Whose Time Has Come," IEEE Comm. Mag., Vol. 31, May 1990, pp. 5–14.
- [3] Transmission and Multiplexing (TM); Access Transmission Systems on Metallic Access Cables; Very High Speed Digital Subscriber Line (VDSL); Part 2: Transceiver Specification, ETSI TS 101 270-2, European Telecommunications Standards Institute, 2001.

- [4] R. van Nee, G. Awater, M. Morikura, H. Takanashi, M. Webster, and K. W. Halford, "New High-Rate Wireless LAN Standards", IEEE Comm. Mag., Vol. 37, Dec 1999, pp. 82–88.
- [5] B. Muquet, Z. Wang, et. Al., "Cyclic Prefixing or Zero Padding for Wireless Multicarrier Transmissions?," IEEE Trans. on Comm., Vol. 50, no 12, Dec 2002, pp. 2136–2148.
- [6] H. Steendam, M. Moeneclaey, "Different Guard Interval Techniques for OFDM: Performance Comparison", in Proc. of MC-SS'07, Herrsching, Germany, May 2007, pp. 11–24.
- [7] A. Onic, M. Huemer, "Direct vs. Two-Step Approach for Unique Word Generation in UW-OFDM," in Proc. InOWo'10, Hamburg, Germany, Sep 2010, pp. 145–149.
- [8] I. S. Reed, G. Solomon, "Polynomial Codes over Certain Finite Fields," Journal of SIAM, Vol 8, no 2, 1960, pp. 300–304.
- [9] C. Hofbauer, M. Huemer, J. B. Huber, "Coded OFDM by Unique Word Prefix," In Proc. ICCS'10, Singapore, Nov 2010.
- [10] W.Y. Zou, Yiyang Wu, "COFDM: an Overview," IEEE Trans. on Broadcasting, Vol. 41, no.1, Mar 1995, pp. 1 - 8.
- [11] Z. Liu, Y. Xin, and G. B. Giannakis, "Linear Constellation Precoding for OFDM with Maximum Multipath Diversity and Coding Gains," IEEE Trans. on Communications, Vol. 51, no 3, Mar. 2003, pp. 416–427.
- [12] Y.-P. Lin and S.-M. Phoong, "BER Minimized OFDM Systems with Channel Independent Precoders," IEEE Trans. on Signal Processing, Vol. 51, no 9, Sep. 2003, pp. 2369–2380.
- [13] H. Steendam, "Analysis of the Redundant Energy in UW-OFDM," submitted to IEEE Trans. on Comm.